

**NIST Measurement Services:**

---

**Measurement Assurance Program for  
Wavelength Dependence of  
Polarization Dependent Loss in Fiber  
Optic Devices over the Wavelength  
Range from 1535 nm to 1560 nm**

**NIST  
Special  
Publication  
250-60**

**Rex M. Craig  
Chih-Ming Wang**

**NIST**

**National Institute of Standards and Technology**  
Technology Administration, U.S. Department of Commerce

NIST Special Publication 250-60

# **NIST MEASUREMENT SERVICES:**

Measurement Assurance Program for Wavelength  
Dependence of Polarization Dependent Loss in Fiber  
Optic Devices over the Wavelength Range from  
1535 nm to 1560 nm

Rex M. Craig

**Optoelectronics Division**

*Electronics and Electrical Engineering Laboratory  
National Institute of Standards and Technology  
325 Broadway  
Boulder, CO 80305*

Chih-Ming Wang

**Statistical Engineering Division**

*Information Technology Laboratory  
National Institute of Standards and Technology  
Boulder, CO 80305*

February 2003



U.S. Department of Commerce  
*Donald L. Evans, Secretary*

Technology Administration  
*Phillip J. Bond, Under Secretary of Commerce for Technology*

National Institute of Standards and Technology  
*Arden L. Bement, Jr., Director*

**National Institute of Standards and Technology Special Publication 250-60**  
**Natl. Inst. Stand. Technol. Spec. Publ. 250-60, 44 pages (February 2003)**  
**CODEN: NSPUE2**

**U.S. GOVERNMENT PRINTING OFFICE**  
**WASHINGTON: 2003**

For sale by the Superintendent of Documents, U.S. Government Printing Office  
*Internet:* bookstore.gpo.gov — Phone: (202) 512-1800 — *Fax:* (202) 512-2250  
*Mail:* Stop SSOP, Washington, DC 20402-0001

# Contents

<b>1. Introduction.....</b>	<b>1</b>
<b>2. MAP Process Outline.....</b>	<b>2</b>
<b>3. MAP Transfer Standard Description and Design.....</b>	<b>2</b>
<b>4. MAP Transfer Standard Implementation.....</b>	<b>4</b>
<b>5. Uncertainties Associated with a MAP Transfer Standard.....</b>	<b>5</b>
<b>5.1. Uncertainty in PDL<sub>1</sub> at Fixed Temperature.....</b>	<b>5</b>
<b>5.2. Uncertainty due to Temperature Dependence of PDL<sub>1</sub>.....</b>	<b>6</b>
<b>5.3. Uncertainty Due to Large Thermal Variations During Shipping.....</b>	<b>8</b>
<b>5.4. Uncertainty Due to Connector/Photodetector PDL.....</b>	<b>8</b>
<b>5.5. Uncertainties Associated with Source Characteristics.....</b>	<b>9</b>
<b>6. Summary.....</b>	<b>10</b>
<b>7. References.....</b>	<b>11</b>
<b>Appendix A, Assurance Procedure for the PDL<sub>1</sub> MAP.....</b>	<b>13</b>
<b>Appendix B, The PDL<sub>1</sub> Measurement System and Selected MAP Results .....</b>	<b>15</b>
<b>Appendix C, Qualification of Artifacts and Measurement System.....</b>	<b>31</b>
<b>Appendix D, Uncertainties Associated with All-States Measurement.....</b>	<b>33</b>
<b>Appendix E, Sample PDL<sub>1</sub> Certificate.....</b>	<b>35</b>
<b>Appendix F, Effect of Source Spectral Symmetry.....</b>	<b>43</b>
<b>Appendix G, Shipping and Handling Instructions.....</b>	<b>45</b>
<b>Appendix H, PDL<sub>1</sub> Artifact Tray/MM Depolarizer Mount.....</b>	<b>47</b>

### **Abstract**

This paper provides the documentation to establish a Measurement Assurance Program (MAP) using an optical fiber diattenuator for the calibration of polarization-dependent loss (PDL) across the range of telecommunication wavelengths from 1535 to 1560 nm. This MAP transfer standard (or artifact) is based on an all fiber design with well-characterized PDL as a function of wavelength and temperature. This MAP is intended for the calibration of PDL measurement equipment, and is not intended for the simulation of PDL in actual systems. This document details the uncertainty analysis, certification procedure and suggested use for the MAP.

Keywords: polarization dependent loss, PDL; diattenuator, fiber optic; measurement assurance program, wavelength division, WDM, Mueller matrix, spectral dependence, wavelength-dependence

*Important Note: The user of the MAP artifact is referred to Appendix E for specific details and instructions concerning handling and usage of the device.*

## Introduction

Polarization-dependent loss references are important to support high-bandwidth optical fiber networks. As network bandwidth is increased, either by increasing modulation rates or by multiplexing channels in the wavelength or time domains, performance begins to suffer as a result of systematic effects that include polarization dependence. Polarization dependence manifests itself in a variety of ways that are commonly interrelated and includes polarization-dependent (insertion) loss (PDL) of components, polarization-dependent gain (PDG) of amplifiers, polarization-dependent response of photoreceivers, polarization-dependent center-wavelength shift (PDW) of narrow filters, and polarization-mode dispersion (PMD) in components and fiber. Of these measurements, the first three can be calibrated by the PDL reference described here.

PDL is defined as  $10 \log(T_{\max}/T_{\min})$  (in dB), where  $T_{\max}$  and  $T_{\min}$  are the maximum and minimum transmittances over the entire polarization state space. With the advent of wavelength-division multiplexed (WDM) fiberoptic communication systems, we have the additional complexity of wavelength dependence of PDL ( $\text{PDL}(\lambda)$ , hereafter referred to as  $\text{PDL}_\lambda$ ). In a WDM system, many wavelength channels are present in the same fiber, thereby increasing the bandwidth of the system by the number of channels.  $\text{PDL}_\lambda$  manifests itself as a statistical noise source in each of these channels.  $\text{PDL}_\lambda$  references are therefore needed to calibrate instruments that characterize WDM components.

This Measurement Assurance Program (MAP) transfer standard is an optical fiber diattenuator for the calibration of polarization-dependent loss across the 1535 – 1560 nm range of telecommunication wavelengths. The MAP artifact<sup>1</sup> is an all-fiber design with PDL accurately measured as a function of wavelength and temperature. The artifact is intended for use in the calibration of PDL measurement equipment and is not intended for the simulation of PDL in actual systems, since the output is not single-mode.

Based on our experience with the telecommunications industry, we determined that wavelength-dependent PDL reference values between 0.05 dB and 0.3 dB (with an emphasis at 0.1 dB) would be most useful, as this is the accuracy to which most components and network design models are specified. This document summarizes the design and implementation of the PDL MAP followed by the results of the uncertainty analysis and MAP certification procedure.

---

<sup>1</sup> The terms “artifact”, “standard artifact”, and “transfer standard” are used interchangeably.

Section 3 describes the nature and design of the MAP artifact, while Sec. 4 details implementation. Section 5 outlines the sources of uncertainty and associated analysis for both the MAP artifact and the  $PDL_\lambda$  measurement systems. The results are summarized in Sec. 6.

## **2. MAP Process Outline**

NIST measurement assurance programs can assist in the establishment of NIST traceability for those situations where a limited number of artifactual transfer standards exist. The difference between the MAP program and the SRM program is that the artifact standards are loaned rather than sold. This MAP program allows NIST to measure the standard artifact before and after it is measured by the customer. While there is a sequence of events associated with the use of a MAP artifact, to the user, the end result is similar to that obtained by the use of an SRM, with one exception. That is, the certificate is not given to the customer until after return of the standard artifact to NIST. The sequence of events is outlined in App. A.

## **3. MAP Transfer Standard Description and Design**

A schematic of the MAP artifact is shown in Fig. 1. This all-fiber device provides a wavelength dependent PDL in the range of 0.05 - 0.3 dB (approximate) within a subset (1535 – 1560 nm) of the ITU "C-band" for wavelength multiplexing. The polarization dependence arises from a segment of single-polarization (polarizing or PZ) fiber [1,2] that provides relatively stable PDL over the range of 5 - 40 °C. Polarizing fiber is a special form of polarization-maintaining fiber that maintains a linearly polarized guided mode parallel to its so-called "slow" axis while the orthogonal linearly polarized mode is unguided. The input is a short single-mode section for accurate coupling to system leads. The output section is composed of approximately 40 meters of high-numerical-aperture (NA) multimode fiber that effectively depolarizes the signal, thereby reducing uncertainty due to the added PDL of connectors and detectors that follow. Hot-wire fusion splicing is used to produce clean joints between the dissimilar fibers. Our early experience with the large uncertainties of our own opto-mechanical fiber-pigtailed PDL artifact prototypes led us to conclude that a properly prepared all-fiber design can be more stable over the long-term. Severe thermal or mechanical shocks, however, can shift the value or cause temporary instability.

Another reason for choosing fiber was the importance of simulating wavelength dependent PDL in order to allow calibration of measurement system linearity using broadband tunable sources. Because of its design, polarizing fiber is well suited as a source of wavelength-

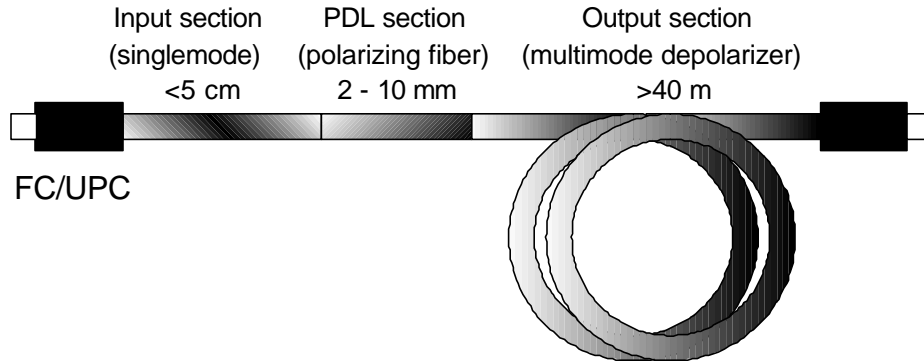


Figure 1. Construction schematic of the MAP artifact detailing the individual fiber components.

dependent PDL [3]. Due to limitations associated with multiple-reflection interference in this design, PDL measurements using high-coherence laser sources do not give reliable results. Rather, tunable filters following broadband sources such as amplified-spontaneous-emission (ASE) or light-emitting-diode (LED) devices are the preferred choice, as the coherence length is suitably short to prevent interference.

An important aspect to the construction of a PDL reference is the fact that the total system PDL due to many small contributions is, to a good approximation, the sum of the individual contributions [4]. In addition, PDL can be introduced by virtually anything in the optical circuit including connectors and photoreceivers. Thus, the relationship of the transfer standard to the measurement system is altered by the means of its connection to the system. Connectors are always an issue in PDL measurements, and consequently angle-polish connectors (APC) are ruled out, despite their superior return loss, due to their inherently high PDL. For PDL repeatability on connection and disconnection, our best results are obtained with high-quality FC/UPC connectors.

The 40 m multimode fiber section following the PDL element is used to mitigate the effect of extraneous PDL in the receiver end of the user's measurement system. The multimode fiber depolarizes the output light, drastically reducing the amount of amplitude modulation (false PDL) induced by PDL in the detector, etc. This is a more practical solution than to merely measure the background PDL of the system because a single-mode output from the MAP artifact



would serve to randomize the alignment between the MAP and the PDL of the detector making it impossible to compensate through a background correction.

#### 4. MAP Transfer Standard Implementation

Photographs of the MAP transfer standard are shown in Fig. 2. The major components are the aluminum fiber tray, diattenuator section (short length of PZ fiber), FC/UPC input connector, the bulkhead mating sleeves, and the multimode-fiber depolarizer loop. The input section is a 5 cm length of common 9/125  $\mu\text{m}$  single-mode (SM) fiber connectorized with a high-quality FC/UPC connector. This section is fusion-spliced to a section of PZ fiber (18 dB/m extinction) whose length (5 – 10 mm) is empirically determined to produce a PDL in the nominal range. The output section consists of a 40 m length of high-numerical-aperture (0.37 NA) multimode (MM)



Figure 2. The completed MAP transfer standard showing both front and top views.

fiber (50/125  $\mu\text{m}$ ) that is fusion spliced to the diattenuator section. The diattenuator section is immobilized and protected by a splice protector that consists of soft silicone rubber tubing and a stainless steel rod inside shrinkable tubing. The splice protector is fixed to the tray with adhesive and the tray is filled with a shock-absorbing silicone gel. The MM depolarizing loop is wound around the base of the tray and terminated with another high-quality FC/UPC connector.

When first constructed, artifacts have only a short length (~25 cm) of MM fiber to simplify initial qualification. Following thermal and optical qualification, these prototypes are then spliced to the depolarizer loop. The completed artifact is then subjected to additional thermal cycling to relieve stresses.

Because there remains some susceptibility to thermal shock, a small battery powered temperature-logging device that monitors a thermocouple connected to the interior is attached to

the rear-facing panel of the enclosure. This logging device is capable of sampling the device temperature over several weeks. This covers time spent in shipment and measurement at a remote location. On return, the logged information is processed to ensure that there were no temperature excursions capable of invalidating the calibration.

## **5. Uncertainties Associated with a MAP Transfer Standard**

There are three primary issues of uncertainty associated with PDL measurements of this MAP. These are the internal uncertainty of the user's measurement system, the external uncertainty introduced by the act of connecting a test specimen, and the uncertainty of the transfer standard itself. The dominant sources of uncertainty in the transfer standard are the calibration, temperature dependence and shipping offsets. We discuss each of these issues below.

### **5.1. Uncertainty in $PDL_{\lambda}$ at Fixed Temperature**

NIST characterizes the wavelength dependence of PDL in these artifacts using the 4-state Mueller/Stokes measurement system designed for this purpose and described in App. B (also a separate publication). Included in the appendix is a detailed uncertainty analysis for measurements done at room temperature (23 °C). The 15 nm single-scan wavelength range is a temporary limitation of the present measurement system and is the region over which the scan wavelength is calibrated dynamically against a portion of an HCN reference cell absorption spectrum (NIST Standard Reference Material (SRM) 2519). Consequently, the  $PDL_{\lambda}$  data combine two scans that, together, span the total range. Figure 3 gives a typical  $PDL_{\lambda}$  scan over the full 1535 – 1560 nm range along with a least-squares fit. Actual  $PDL_{\lambda}$  data at ITU "C-band" grid wavelengths and associated uncertainties accompany each MAP artifact in its Certificate. The combined standard uncertainty [5] of the NIST system over any scan in the 1530 – 1560 nm region at a 0.12 dB reference level<sup>2</sup> is  $u_{MS}(0.12) = 0.0079$  dB (from App. B).

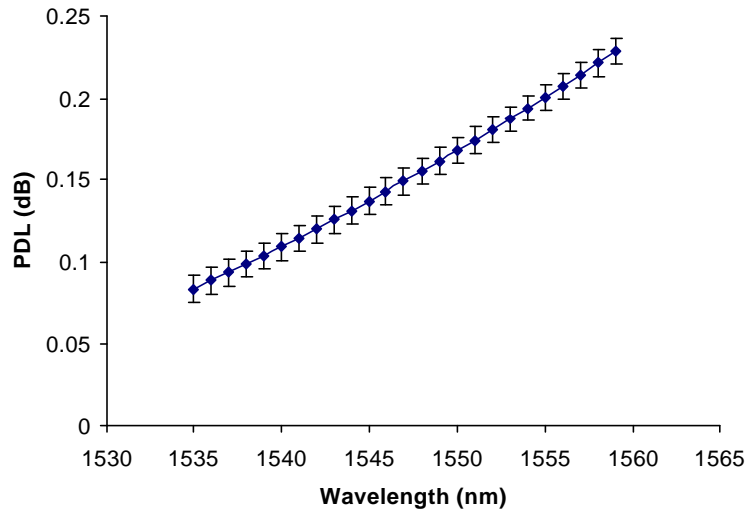


Figure 3. Typical  $PDL_{\lambda}$  data for the MAP standard. Error bars represent the measurement system's standard uncertainty.

## 5.2. Uncertainty due to Temperature Dependence of $PDL_1$

Temperature dependence of  $PDL_{\lambda}$  ( $PDL(\lambda, T)$ ) is characterized over wavelength by a different measurement system based on automated scans over all states of polarization. Wavelength tunability is supplied by a broadband source followed by a tunable filter. A schematic of the test system appears in Fig. 4. It consists of an ASE source followed by a fiber-Fabry-Perot tunable filter (FFP-TF) of 0.7 nm 3 dB bandwidth (Lorentzian profile), a fiber-loop polarization controller, an optical power meter with sampling and averaging capabilities, and the device under test (DUT) enclosed in an environmental test chamber. Because the measurement system is an all-states type, the uncertainties in

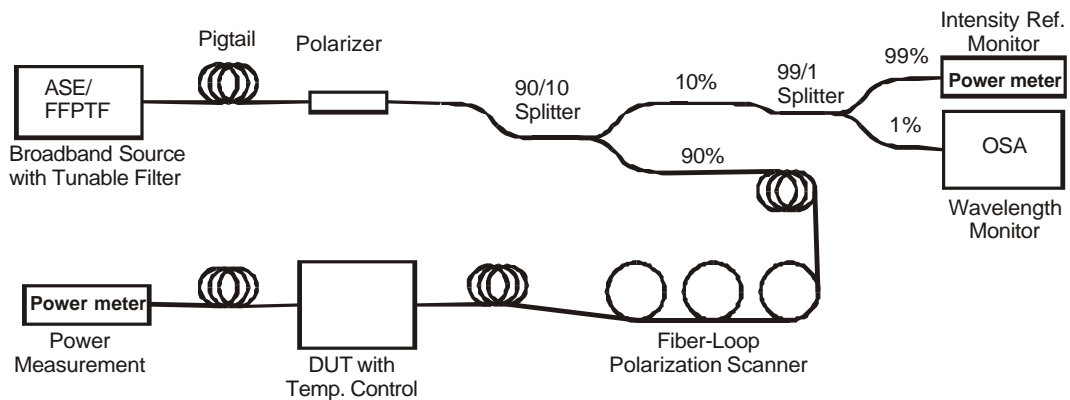


Figure 4. Schematic of the all-states PDL system used for thermal characterization of the  $PDL_{\lambda}$  artifact.

<sup>2</sup> A nominal PDL value of 0.12 dB is used throughout to establish a reference level for uncertainty calculations

PDL at a particular temperature can be characterized in a manner similar to that in [6] with the uncertainty budget given in Table 1 of App. D. If  $T_1$  and  $T_2$  are the maximum and minimum measurement temperatures, the differential temperature coefficient's contribution to uncertainty at a given wavelength can be approximated by  $(PDL(I, T_1) - PDL(I, T_2)) / 2(T_1 - T_2)$ . Figure 5 gives the temperature coefficient data over the 1525 – 1565 nm wavelength range along with a polynomial fit for three artifacts.

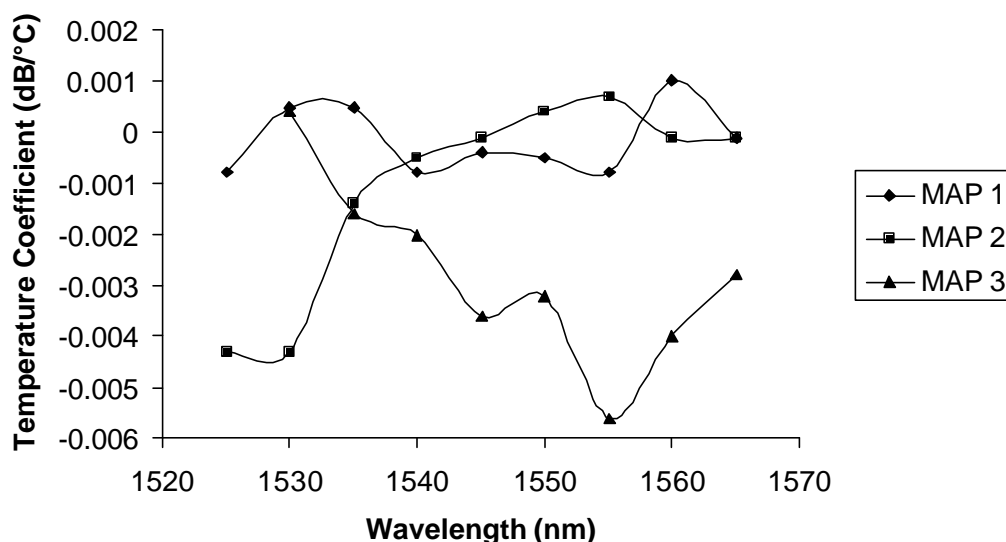


Figure 5. Typical temperature dependence of  $PDL_\lambda$  data for 3 MAP artifacts.

Individual measurements at temperature  $T_1 = 26^\circ\text{C}$  are completed in 10 s and averaged over a group of 20 measurements at each wavelength in 5 nm increments. The temperature is then cycled to  $T_2 = 20^\circ\text{C}$ , and stabilized, and the artifact is measured again. The quoted uncertainty over the range 1535 – 1560 nm range is taken from Fig. 5 to be the maximum absolute value observed in the data (0.0056 dB/°C) multiplied by the user's environmental temperature uncertainty  $\Delta T$ . An environmental temperature uncertainty bound of  $\Delta T = \pm 1^\circ\text{C}$  produces a  $u_T = 0.0056 / \sqrt{3} = 0.0032\text{dB}$  standard uncertainty in  $PDL_\lambda$  [5]. Uncertainty estimates are included in the Certificate for temperature bounds of both  $\pm 1^\circ\text{C}$  and  $\pm 3^\circ\text{C}$ . The choice of bound is determined by the degree of temperature control in the user's measurement environment.

### 5.3. Uncertainty Due to Large Thermal Variations During Shipping

Because these devices may retain some sensitivity to large temperature cycles that can shift  $PDL_\lambda$ , they must be well insulated during shipping and shipped by the most rapid means available. In addition, a logging device will constantly monitor the ambient temperature over the entire span of the trip. NIST will tabulate this data at the end of the calibration cycle to insure that the artifact has not been exposed to temperature extremes (outside the range 0 – 50 °C) that may invalidate the Certificate. The uncertainty has been calculated from observed shifts of wideband PDL values at room temperature following a cycling of the ambient temperature between two extremes that begin over 15 – 35 °C and widen to 0 – 50 °C. Shifts are characterized by a ratio of the PDL standard deviation,  $\sigma_{\text{shift}}$ , over four thermal cycling sequences to the mean PDL,  $\langle PDL \rangle$ , observed. Only devices that maintain a ratio of shift standard deviation to mean ( $\sigma_{\text{shift}}/\langle PDL \rangle$ ) of less than 10% are selected for MAP artifacts. The uncertainty will be taken as the maximum observed ratio. Based on a series of measurements, the maximum of ( $\sigma_{\text{shift}}/\langle PDL \rangle$ ) is 3.7% of wideband PDL, which gives a standard uncertainty of  $u_{\text{ship}}(0.12) = 0.0045$  dB for a 0.12 dB reference PDL value.

### 5.4. Uncertainty Due to Connector/Photodetector PDL

Any connection between two singlemode optical fibers can introduce PDL, whether through Fresnel reflections, lateral core offset, or mode-field mismatch. Thus the artifact is subject to a PDL uncertainty at the input connection. While these uncertainties are generally small with high-quality FC/UPC connectors, only by averaging results over multiple measurement trials with various input leads and connectors can the user reduce input lead contributions. This can be seen by characterizing each PDL contribution as a "vector" (or axis) normal to propagation. This vector determines whether input connector PDL ( $PDL_1$ ) adds or detracts from the internal system PDL ( $PDL_2$ ). The result is approximated by  $\overline{PDL}_{\text{tot}} \cong \overline{PDL}_1(\mathbf{q}_1) + \overline{PDL}_2(\mathbf{q}_2) \cdot \cos(2(\mathbf{q}_1 - \mathbf{q}_2))$  dB where  $\mathbf{q}_1$  and  $\mathbf{q}_2$  represent the angles of PDL vector for the connector and system PDL. When vectors are aligned, the total PDL is the sum of the two. Likewise when the axes are orthogonal the

total approximates the difference. There is no way to determine, *a priori*, the relative angle between the two axes. The user may estimate this uncertainty by sampling system PDL with a variety of input leads and connectors without a DUT in place. One is thus effectively averaging over several axis angles and connector types. The result is a random component to be added in quadrature to the MAP uncertainty rather than an offset to be added directly. At the output of the MAP artifact an accurate calibration requires that this random component be minimized through depolarization. Although the artifact's output depolarizer is not completely effective, the remaining degree-of-polarization (DOP) is small (approximately 5 % for a source bandwidth of 0.7 nm or greater). Consequently any remaining PDL due to output connectors and to photodetectors contributes with only a 5 % weighting, and is negligible.

### **5.5. Uncertainties Associated with Source Characteristics**

Fixed or tunable sources with 3-dB bandwidths between 0.7 and 20 nm are generally appropriate sources for use with the MAP artifact. Certification for larger bandwidths can be accommodated by special request. Examples of appropriate sources include filtered ASE sources, filtered LED sources, and multimode lasers. Narrowband fixed or tunable laser sources cannot be used, in general, due to the prevalence of interference effects generated by high coherence and back-reflection. Interference must be avoided in any precise measurement of PDL since the drift of the associated maxima and minima are often indistinguishable from the PDL signal. A useful alternative is the use of a broad optical source with a narrowband filter that is capable of wavelength dither at high frequencies, such as a fiber-Fabry/Perot design driven by a PZT transducer. The dither is an effective decorrelator if the dither period is low compared to photodetector integration time.

While broadband sources typically exhibit a low degree of polarization, this may not always be true. A common source of false PDL signals is a partially polarized source followed by singlemode fiber and a polarizer positioned prior to a polarization controller. Drift in fiber birefringence causes the polarized component of the source to wander over all states, producing erroneous intensity fluctuations on the output of the polarizer. Consequently, the user should recognize this and ensure that the source is

well depolarized with degree-of-polarization generally less than 1% unless the source and polarizer are separated by only a very short, stable length of intervening fiber. The alternative is source-intensity normalization through a ratio incorporating a second power monitor prior to the polarization controller, as in Fig. 4.

Finally, the user should be aware that the measured PDL, using a broadband source symmetric in wavelength, is the integrated  $PDL_\lambda$  over the source bandwidth. For sufficiently narrow sources, the measured PDL is the source-center-wavelength value. The effect of source spectral asymmetry is discussed in App. F.

## 6. Summary

The standard uncertainties described in sections 5.1 to 5.4 above are added in quadrature and multiplied by a coverage factor of 2 [5] to yield the expanded uncertainty included in the Certificate. PDL uncertainties due to the customer's connections should be estimated separately as outlined above and then added in quadrature to the expanded uncertainty.

A description of the NIST 4-state Mueller/Stokes measurement system appears in App. B. The qualification procedure for the MAP appears in App. C, and uncertainties associated with all-states measurement are given in App. D. A sample MAP certificate is presented in App. E. The certificate includes the certified  $PDL_\lambda$ , along with the associated standard uncertainties for two different temperature uncertainties about room temperature (23 °C), and instructions for use of MAP transfer standard. The actual MAP certificate will be sent to the user following a MAP measurement. A cautionary description of the effect of asymmetric source spectra is given in App. F. Finally, shipping instructions are included in App. G, and a schematic diagram of the aluminum tray/spool assembly appears in App. H.

## 7. References

1. M. J. Messerly *et al.*, "A broad-band single polarization optical fiber," *J. Lightwave Technol.*, vol. 9, pp. 817 – 820, 1991.
2. K. Tajima *et al.*, "A new single-polarization optical fiber," *J. Lightwave Technol.*, vol. 7, pp.1499 - 1503, 1989.
3. M. J. Messerly, R. E. Budewitz and B. K. Nelson, "Characterization of single polarization fiber," *Tech. Digest – Symposium on Optical Fiber Meas.*, NIST Special Publication 864, 1994, pp. 185 – 188, 1994.
4. N. Gisin, "Statistics of PDL," *Opt. Comm.*, vol. 114, pp. 399-405, 1995.
5. B. N. Taylor and C. E. Kuyatt, "Guidelines for evaluating and expressing the uncertainty of NIST measurement results", Tech. Note 1297, *Nat. Inst. Stand. Technol.*,, 1994.
6. Hewlett-Packard Product Note, "Polarization-dependent loss measurements using modular test system configurations", PN-11896-1, 4/95



## Appendix A

### **Assurance Procedure for the PDL<sub>1</sub> MAP**

1. NIST performs calibration of its Mueller/Stokes PDL system using the BK7<sup>3</sup> reference.
2. NIST performs calibration of its All-States PDL system using the BK7 reference.
3. NIST performs initial temperature coefficient measurements of MAP unit.
4. NIST measures MAP unit using Mueller Stokes technique.
5. NIST initializes temperature logger and packs unit prior to shipping.
6. NIST ships unit to customer.
7. Customer measures PDL of unit and ships it back to NIST within 4 – 6 weeks, if possible.
8. NIST receives unit.
9. NIST unpacks unit and analyzes temperature logger for exposure to temperatures outside 0 °C – 50 °C range.
10. NIST runs final Mueller/Stokes measurement of MAP unit.
11. NIST runs final temperature-coefficient measurements.
12. On verification that all parameters are within specification, NIST mails certificate to customer.

---

<sup>3</sup> Certain materials and equipment are identified in this paper to foster complete understanding. Such identification does not imply recommendation or endorsement by NIST, nor does it imply the materials or equipment are necessarily the best available.

## Appendix B (Preliminary)

### **The PDL<sub>1</sub> Measurement System and Selected MAP Results**

*Abstract* – Building on previous work, a rapid, automated, non-mechanical measurement system for spectral characterization of polarization-dependent loss (PDL) has been developed. A deterministic fixed-states Mueller/Stokes method in conjunction with real-time calibrated spectral information is used to derive wavelength-dependent Mueller matrix elements. Voltage-modulated liquid-crystal variable retarders set the input polarization states. A narrow, voltage-tuned filter provides a wavelength sweep following a broadband source; the sweep wavelength is calibrated in real-time by hydrogen-cyanide reference lines. This rapid measurement system can measure PDL over a wavelength range of 15 nm in 5 seconds. A complete uncertainty analysis has been conducted for PDL in the range of 0.05 to 0.3 dB with an expanded uncertainty of 0.0098 dB over the range from 1535 to 1560 nm. Performance was verified with a Fresnel reference. Finally, design and performance results from all-fiber artifact calibration standards are presented.

#### **1. Introduction**

Until the advent of dense wavelength-division multiplexing (DWDM) systems, polarization-dependent loss (PDL) was usually characterized at only a specific wavelength [1]. More recently, however, the wavelength dependence of PDL ( $PDL(\lambda)$ , hereafter referred to as  $PDL_\lambda$ ) has assumed greater importance, particularly in component metrology. A modification of a previously reported, deterministic fixed-states technique [2] has been implemented that allows PDL to be characterized as a function of wavelength. The goal is to establish a capability for rapid measurement of  $PDL_\lambda$  to a resolution finer than 0.005 dB without sacrificing accuracy. This approach uses a non-mechanical matrix technique employing ratio detection and simultaneous spectral calibration via a hydrogen-cyanide (HCN) reference that is faster than most tunable-laser systems (taking only 5 seconds for a 15 nm range) and more accurate than techniques based on optical spectrum analyzers [3]. In addition, this approach can be customized to the resolution requirements of both wideband and narrowband devices. Wideband devices such as switches, commonly exhibit a small variation in  $PDL_\lambda$  that doesn't require a fine wavelength resolution. In contrast, a narrow-channel device such as a filter may exhibit relatively small values of  $PDL_\lambda$  over the transmission (or reflection) band but large values at the

## Appendix B (Preliminary)

band edge. This type of device requires higher wavelength resolution for accurate characterization.

New results from an all-fiber  $PDL_\lambda$  artifact reference are also presented. This artifact is intended to become a NIST Measurement Assurance Program (MAP) transfer standard with PDL values in the range of 0.05 – 0.3 dB for the calibration of PDL measurement instrumentation.

In Sec. 2 the concept of the measurement method is discussed, and Sec. 3 describes the experimental implementation. Section 4 outlines a comprehensive uncertainty analysis.

### 2. Concept

Our method is a further variation of a matrix technique, sometimes referred to as the Mueller/Stokes technique, developed by Favin, Nyman and Wolter [4],[5] and modified by Craig et al. [2]. The method relies solely on measurements of power ratio at specific polarization states, but has now been extended to accurately cover a range of wavelengths. As in reference [2], four well-defined polarization states are necessary to determine the first-row Mueller matrix elements of a component. Diattenuation, the global polarization dependence of transmittance, can be determined from these (wavelength-dependent) matrix elements. Because the measurement depends only on the relative coordinates of the four states, the sole requirements on the set are that they maintain relative angular separations of  $90^\circ$  (orthogonality) about the origin of the polarization Poincaré sphere, as shown in Fig. 1. Thus any constant retardance in the measurement path will not affect the measured PDL, since pure retardance does not alter the orthogonality of the states, but merely rotates them uniformly on the sphere. Measurement-

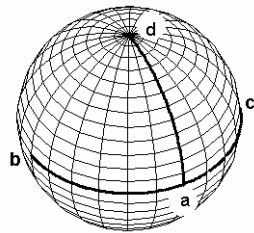


Figure 1a

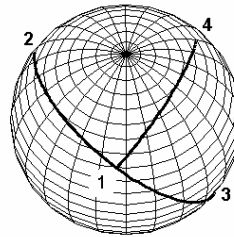


Figure 1b

Fig.1a: Initial Poincaré sphere trajectories of the liquid-crystal variable retarder (LCVR) state generators.  
Fig. 1b: LCVR trajectories following birefringent displacement

## Appendix B

(Preliminary)

system PDL in conjunction with retardance, however, modifies this scenario somewhat by altering the relationship between the launched states and can potentially introduce significant uncertainty. This uncertainty and its resolution will be discussed in detail in section 4.

In the Mueller/Stokes technique, PDL is measured by launching four orthogonal polarization states into the device-under-test (DUT) and for each state, measuring the ratio of the transmitted power ( $I_{T1}(\lambda)\dots I_{T4}(\lambda)$ ) to the launched power ( $I_{L1}(\lambda)\dots I_{L4}(\lambda)$ ). Including the wavelength dependence of these powers, the first row of Mueller matrix elements can be defined from Ref. [2] as

$$\begin{bmatrix} m_{11}(\mathbf{I}) \\ m_{12}(\mathbf{I}) \\ m_{13}(\mathbf{I}) \\ m_{14}(\mathbf{I}) \end{bmatrix} = \begin{bmatrix} \frac{1}{2} \left[ \frac{I_{T1}(\mathbf{I})}{I_{L1}(\mathbf{I})} + \frac{I_{T2}(\mathbf{I})}{I_{L2}(\mathbf{I})} \right] \\ \frac{1}{2} \left[ \frac{I_{T1}(\mathbf{I})}{I_{L1}(\mathbf{I})} - \frac{I_{T2}(\mathbf{I})}{I_{L2}(\mathbf{I})} \right] \\ -\frac{1}{2} \left[ \frac{I_{T1}(\mathbf{I})}{I_{L1}(\mathbf{I})} + \frac{I_{T2}(\mathbf{I})}{I_{L2}(\mathbf{I})} \right] + \frac{I_{T3}(\mathbf{I})}{I_{L3}(\mathbf{I})} \\ -\frac{1}{2} \left[ \frac{I_{T1}(\mathbf{I})}{I_{L1}(\mathbf{I})} + \frac{I_{T2}(\mathbf{I})}{I_{L2}(\mathbf{I})} \right] + \frac{I_{T4}(\mathbf{I})}{I_{L4}(\mathbf{I})} \end{bmatrix}. \quad (1)$$

The spectral transmittance extrema,  $T_{\min}(\lambda)$  and  $T_{\max}(\lambda)$  are obtained from the matrix elements above by optimization as

$$\begin{aligned} T_{\max}(\mathbf{I}) &= m_{11}(\mathbf{I}) + \sqrt{m_{12}(\mathbf{I})^2 + m_{13}(\mathbf{I})^2 + m_{14}(\mathbf{I})^2} \\ T_{\min}(\mathbf{I}) &= m_{11}(\mathbf{I}) - \sqrt{m_{12}(\mathbf{I})^2 + m_{13}(\mathbf{I})^2 + m_{14}(\mathbf{I})^2}, \end{aligned} \quad (2)$$

so that

$$PDL_I \equiv PDL(\mathbf{I}) = 10 \log \left[ T_{\max}(\mathbf{I}) / T_{\min}(\mathbf{I}) \right]$$

holds globally over the entire space of polarization states and wavelength.

Errors due to  $PDL_\lambda$  internal to the measurement system and the wavelength dependence of the liquid-crystal variable retarders (LCVR) are dramatically reduced through normalization of DUT input and output powers in two separate ratios. This arrangement virtually eliminates fluctuations in source power, common-mode drift, spectral dependence in the measurement system and system  $PDL_\lambda$ . In the first normalization, four initial ratio measurements  $I_{T1}(\mathbf{I})\dots I_{T4}(\mathbf{I})$  are taken that are in fact signal-to-reference ratios without the DUT in place, while the final four

## Appendix B (Preliminary)

measurements  $I_{L_1}(\mathbf{I}) \dots I_{L_4}(\mathbf{I})$  are signal-to-reference ratios with the DUT in place. These ratios remove spectral dependence in various elements of the system as well as source fluctuations and common-mode drift. The second normalization is simply the ratio of  $I_T$  and  $I_L$  as used in Eq. 1 above; this removes the inherent  $\text{PDL}_\lambda$  of the system so that only the  $\text{PDL}_\lambda$  of the DUT remains.

### 3. Implementation

Figure 2 shows a schematic of the measurement system. The system consists of three major sections: (1) an amplified, spontaneous-emission (ASE) source with a tunable, filtered output calibrated against a NIST wavelength reference, (2) the LCVR polarization state generator, and (3) a measurement section.

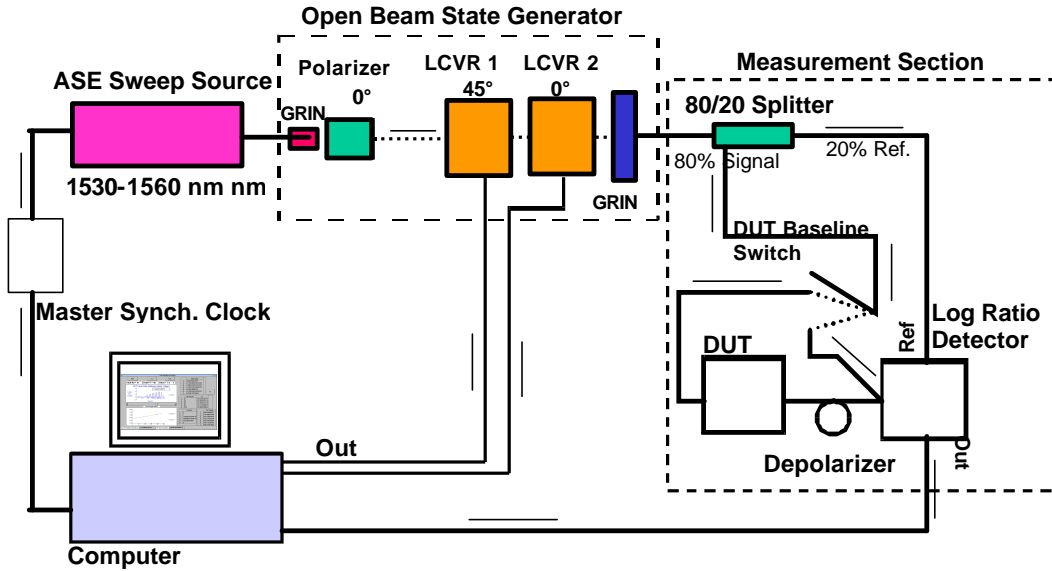


Figure 2: Simplified diagram of the measurement system

*Light source and wavelength calibration:* The ASE source in Fig. 3 is of a spectrally flattened NIST design followed by a fiber-Fabry-Perot tunable filter (FFP-TF) tunable over the ASE range from 1535 – 1560 nm with a full-width-at-half-maximum (FWHM) bandwidth of 0.7 nm and a free-spectral-range of 85 nm. The FFP-TF is driven by a ramp-generator circuit in a repetitive sweep that is triggered by signals from the control computer. The FFP-TF output is tapped by two 10/90 wavelength-independent couplers in series. The first directs 10 % of the light through a NIST HCN wavelength reference (Standard Reference Material (SRM) 2519) [6] to one input

Appendix B  
(Preliminary)

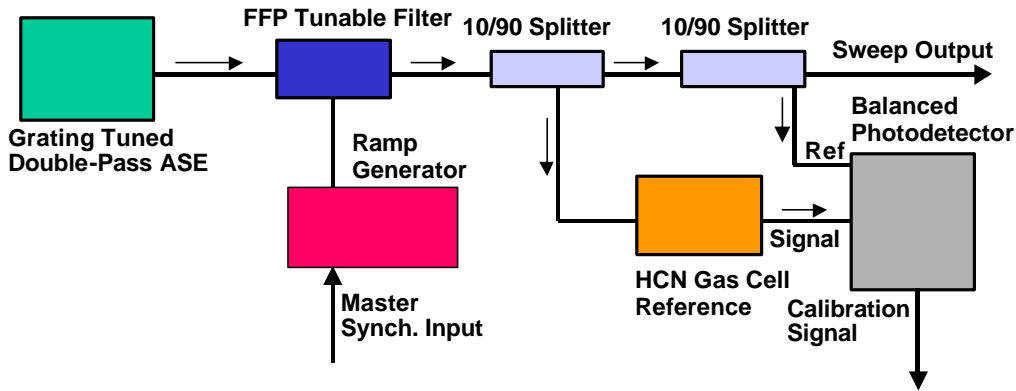


Figure 3: Diagram of swept wavelength source with HCN calibrator (Sweep

of a balanced differential InGaAs photoreceiver. The second directs 9 % of the light to the other input of the differential photoreceiver to act as a source-level reference. The differential photoreceiver produces an HCN absorption spectrum that acts as a calibration signal with 50 dB of common-mode rejection. This calibration signal is sampled to 16-bit resolution by the control computer and logged. The absorption peaks were fitted by a least-squares quadratic fit and compared to the known peak wavelengths following each scan, providing near real-time spectral calibration of each sample point. This calibration signal appears in Fig. 4. Presently, each sweep spans only 15 nm of the range from 1535 – 1560 nm because of speed and sampling-density constraints related to HCN calibration; a full span of 25 nm must be covered in at least two steps. The 0.7 nm Lorentzian bandwidth  $\Delta\lambda$  of the source at  $\lambda = 1550$  nm gives a coherence length

$$l_c = \lambda^2 / \Delta\lambda \cong 1.1 \text{ mm} . \quad (3)$$

This coherence length is insignificant compared to the typical distances (of order 1 cm) between uncoated surfaces in the measurement system, so multiple reflection interference is minimized.

*Polarization-state generation:* The major portion of the swept-source output light is collimated by a GRIN lens and then passed through a Glan-Thompson polarizer followed by a series of two LCVR units used to generate the four polarization states. An LCVR is a liquid crystal element whose retardance can be controlled by an applied voltage. The first LCVR, with fast axis at  $45^\circ$  to the incident polarization, provides either zero or half-wave retardance. The second LCVR, with fast axis at  $0^\circ$ , provides either zero or quarter-wave retardance. Polarization modulation is synchronized with each source wavelength sweep in the sense that each state setting triggers a new spectral sweep.

## Appendix B (Preliminary)

The choice of sweep priority, (i.e., each polarization state having its own wavelength sweep rather than the launching of each of four states at every wavelength of a single spectral sweep)

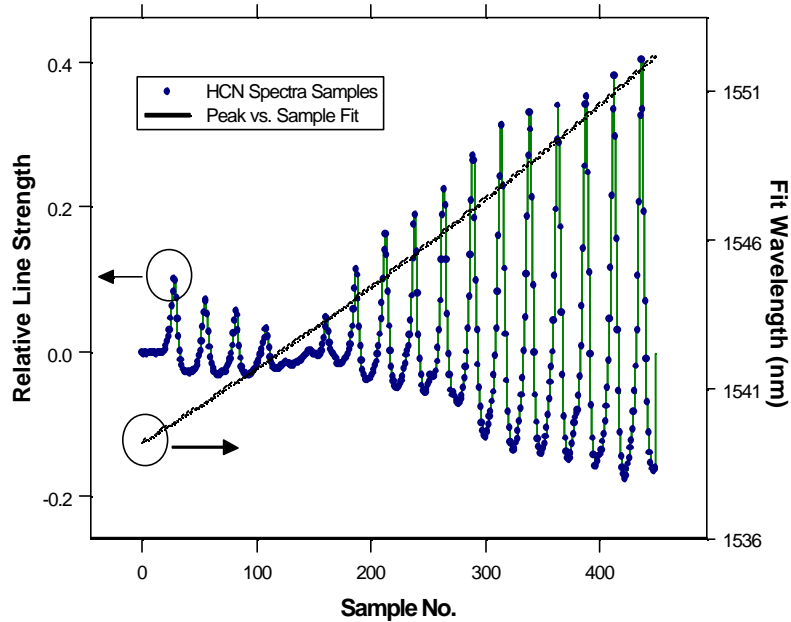


Figure 4: Typical P-branch HCN absorption signature from 1539 to 1551 nm with a quadratic calibration fit

was made because it allows rapid spectral calibration. Each spectral sweep was sampled at a rate sufficient to resolve HCN absorption peaks to the required accuracy. The spectral data for each polarization state are aligned in wavelength. Voltages are generated by the control computer and synchronized to the source sweep by a master-clock-modulated LCVR retardance. Retardance modulation was checked periodically against a polarimeter to ensure the proper relationship among the four states. After the second LCVR, a pigtailed GRIN lens launches the polarization-modulated light back into single-mode fiber connected to a spectrally flattened 80/20 splitter.

*Measurement and calibration:* Transmitted and launched powers were measured respectively with and without the DUT in place, c.f. Fig. 2. The 80/20 splitter was used followed by a ratio detector to obtain the  $I_T$  and  $I_L$  ratios to source power (removing effects of drift). The major portion (80 %) of the splitter output can be switched between the DUT and a direct connection to the first input of a second balanced differential photoreceiver to establish a measurement baseline. The system calibration was checked by replacing the DUT with a fiber-pigtailed open-

## Appendix B (Preliminary)

beam cavity containing a polished BK-7<sup>4</sup> glass block. The block can be tilted to vary the Fresnel reflections in a predictable way to emulate a PDL. Calculated (Fresnel) and measured PDL values as a function of input angle are presented in Fig. 5 and agree to  $\pm 0.005$  dB. The residual system PDL was measured at  $0^\circ$  (normal incidence) as a  $0.0014 \pm 0.0006$  dB offset over all wavelengths. A residual slope indicates a small systematic uncertainty since BK7 has negligible dispersion over this range.

Finally, the DUT  $\text{PDL}_\lambda$  signal was sampled at 450 points for each 15 nm wavelength scan. A

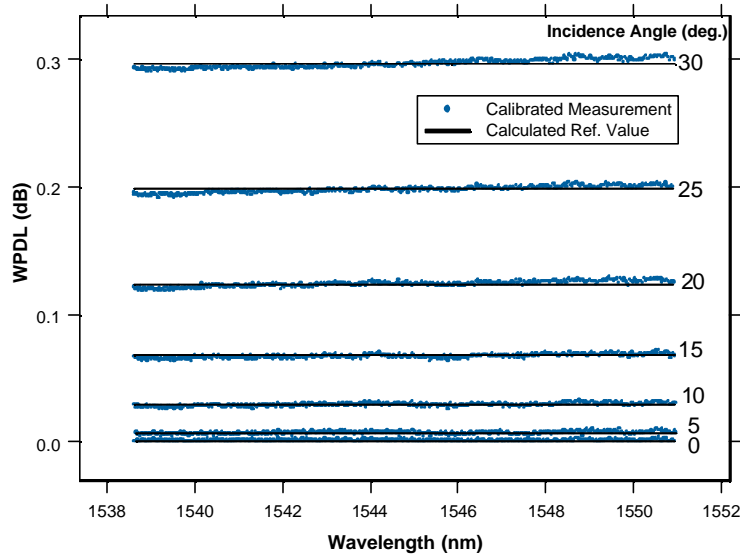


Figure 5: Open-beam BK7 artifact data calibrated at  $30^\circ$  incidence. Centerline is the calculated  $\text{PDL}_\lambda$  value. Residual wavelength slope falls within  $2\sigma$  uncertainty.

scan period of 285 ms was required for each polarization state, after which the state was changed to the next in the series. An entire  $\text{PDL}_\lambda$  scan over the 15 nm range takes less than 5 seconds.

### 4. Uncertainties

The design of this measurement system is both simpler and more sophisticated than that described in Ref. [2], in that taking appropriate ratios of key parameters now reduces most uncertainties. Items 1, 2, 3, and 4 below outline the four major systematic uncertainties in polarization and power that, together, comprise the total systematic contributions. The remaining random uncertainties are listed in order of decreasing impact. Values listed correspond to one standard deviation at 1545 nm. The uncertainty analysis is guided by [7].

---

<sup>4</sup> The identification is made to adequately describe the experimental procedure and is not an endorsement by the National Institute of Standards and Technology nor does it imply that the material is the best available for this use.



## Appendix B (Preliminary)

- **Type B Components [7]**

1. *Polarization-state accuracy.* Launched polarization states were measured using a polarimeter. Polarization state accuracy depends on both the polarimeter and the LCVR bias calibration. In this case, the polarimeter has been calibrated (open beam) for three linear states and one circular state by means of a 60-dB extinction Glan-Thompson polarizer followed by a NIST quarter-wave retardance reference [8]. The retardance reference is certified to  $0.1^\circ$  uncertainty at 1300 nm and has  $0.2^\circ$  uncertainty for low-coherence sources out to 1560 nm. The angular resolution for alignment of these two optical elements is  $0.02^\circ$ , a negligible contribution. The associated contribution to uncertainty is the total calibration uncertainty of all four states generated by the pair. Polarimeter/LCVR system measurements are repeatable to 0.06 % ( $0.1^\circ$ ) over linear state angles and to 0.6 % ( $0.5^\circ$ ) in ellipticity over the Poincaré sphere at 1545 nm. Following the polarimeter calibration, the LCVR bias was adjusted at 1545 nm to match the calibration states to within approximately 2.0 %. However, a small systematic offset in the ellipticity of the LCVR circular state of 3.0 % remained. The resulting root-sum-of-squares (RSS) PDL standard uncertainty contribution was 1.2 % (in dB) for each of the linear states and 2.1 % for the circular state.
2. *Retarder wavelength dependence.* The same drive voltage was used on each LCVR state regardless of wavelength, and this causes an uncertainty in the polarization states due to the LCVR wavelength dependence. Based on wavelength-dependent retardance measurements supplied by the vendor, the retardance exhibits only a simple inverse dependence on wavelength  $\lambda$  as  $f_{VR} = 2p\Phi_f(V, T) / \lambda$  where  $\Phi_f(V, T)$  is the LCVR phase delay (in nm) as a function of voltage V and temperature T. The associated uncertainty contribution is:  $(\Delta f_{VR})_{\lambda} = 2p\Phi_f(V, T)\Delta\lambda / \lambda^2$ , where a wavelength scan of  $\Delta\lambda = 10 \text{ nm}$  about  $\lambda = 1550 \text{ nm}$  produces a normalized standard uncertainty of  $\Delta f_{VR} / f_{VR} = 0.35\%$ . This uncertainty is manifested primarily as an uncertainty in the accuracy of each Stokes

## Appendix B

(Preliminary)

state and its associated matrix element. This uncertainty could be reduced through the use of a look-up table.

3. *Retarder temperature dependence* The LCVR retardance has an uncertainty due to

temperature of:  $(\Delta \mathbf{f}_{VR})_T = \frac{2\mathbf{p}}{\mathbf{1}} \frac{\partial \Phi_f(V, T) \Delta T}{\partial T}$ , where the vendor's estimate of

$\partial \Phi_f / \partial T$  is 0.004 nm/°C. A temperature variation of 0.5 °C ( $\Delta T$ ) gives a normalized standard uncertainty contribution of  $(\Delta \mathbf{f}_{VR})_T / \mathbf{f}_{VR} = 0.12\%$  for our conditions.

4. *System internal PDL.* The LCVR elements contribute their own PDL (0.02 dB) to that of the DUT. This manifests itself as a change in intensity with a change in polarization state. This PDL was assumed constant during both phases of the measurement and is cancelled in the normalization ratios. However, any variation in system PDL over the course of a measurement appears as an uncertainty in signal power. Given the maximum observed drift of the internal PDL of 0.02 dB over intervals of 5 minutes, this yielded a PDL standard uncertainty due to LCVR elements of 0.015 %.

***Propagated measurement system uncertainty.*** The element percentages above, inherent to the measurement system, are adjusted standard uncertainties that assume a rectangular distribution [7]. From these values, an error-propagation model based on the defining equations (Eq. 1) produces a Type B standard uncertainty of 0.0047 dB at a reference PDL value of 0.12 dB.

- **Type A Components [7]**

1. *PDL measurement repeatability.* Effects that can be considered statistical in nature include possible coherent interference at the photoreceiver, calibration-spectral-peak registration uncertainty and resulting fit uncertainty, and photoreceiver noise. The combined effect is encompassed by a measurement of system repeatability. Ten undisturbed measurements of a 0.12 dB BK-7 PDL<sub>λ</sub> were made following the initial baseline measurement. The standard deviation of these measurements averaged over all wavelengths yielded 0.0012 dB as the effective standard uncertainty of single-

## Appendix B (Preliminary)

sweep system noise and incorporates all effects such as optical interference and detector noise that average down over multiple measurements.

**Combined standard uncertainty for the measurement system.** The Type A and Type B components above are assumed uncorrelated, so their root-square-sum (RSS) at the 0.12 dB level is an uncertainty  $u_{\text{sys}} = \sqrt{(0.0012^2 + 0.0047^2)} \text{ dB} = 0.0049 \text{ dB}$  for an open-beam PDL measurement. Using a coverage factor ( $k = 2$ ), the **expanded uncertainty** [7] follows as  $2u_{\text{sys}} = 0.0098 \text{ dB}$ .

### • Type A Artifact Contributions

1. *Birefringence-effect uncertainty.* When measuring devices with significant birefringence in the path (fiber pigtailed etc.), the uncertainty associated with 4-state measurements has been calculated to be a variation of 4.5% about the mean of measured  $\text{PDL}_\lambda$  in dB. This value is derived from a computer model (to be discussed in a future publication) of four-state measurements in the presence of multiple PDL sources linked by birefringent fiber. At the 0.12 dB PDL reference value, this uncertainty is 0.0054 dB.
2. *Connector uncertainty.* As in reference [2], a significant source of uncertainty that is not inherent to the LCVR system is variations in measured PDL of DUT artifacts with connectorized pigtailed following disconnection and reconnection. This could be explained by connector alignment (core offset) errors. We have measured this uncertainty to be 0.0029 dB for connectorized artifacts.

**Combined standard uncertainty for the measurement artifact.** Summing the uncorrelated artifact contributions above, the total RSS is  $u_{\text{DUT}} = \sqrt{(0.0054^2 + 0.0029^2)} \text{ dB} = 0.0061 \text{ dB}$  at the 0.12 dB level. Note that this uncertainty is present in any Mueller/Stokes 4-state measurement of PDL.

**Total Combined Standard Uncertainty.** The RSS total of all previous uncertainty contributions is then  $u_{\text{MS}} = \sqrt{(u_{\text{sys}}^2 + u_{\text{DUT}}^2)} = \sqrt{(0.0049^2 + 0.0061^2)} \text{ dB} = 0.0079 \text{ dB}$ , which

## Appendix B (Preliminary)

represents the uncertainty in a typical measurement. The expanded uncertainty is then  $2u_{MS} = 0.016$  dB.

- **Wavelength Calibration Uncertainty.** Based on sampling density, the wavelength uncertainty is estimated to be 0.025 nm for the 0.7 nm FWHM bandwidth of the tunable filter element. For wideband devices in which PDL is constant or varies slowly with wavelength, this uncertainty is not significant. For narrowband devices such as filters, however, this uncertainty may be significant. This value enters the artifact uncertainty in a product with the slope of  $PDL_{\lambda}$ .

Stress and thermal drifts in optical fiber birefringence must be minimized over the course of a measurement. The measurement method is sensitive to small errors in the matrix elements, such as those due to retardance drift between the baseline and DUT measurement. For this reason, one should use short, straight leads anchored to a fixed surface, and calibrate the system prior to each series of measurements.

### 5. All-Fiber PDL Artifact Results

A series of all-fiber PDL artifacts has been constructed (Fig. 6) to aid in the establishment of a NIST  $PDL_{\lambda}$  transfer standard,. These artifacts consist of three sections: single-mode (SM), polarizing (PZ), and multimode (MM) fiber, fusion-spliced together to generate PDL in the range of 0.05 dB – 0.3 dB over the ITU C-band. The PDL section consists of 5 – 10 mm of polarizing

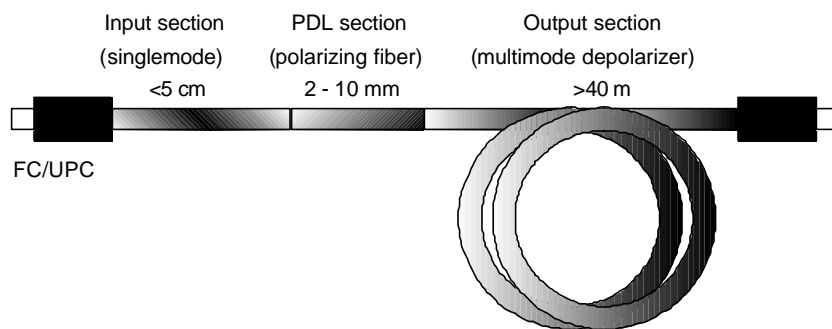


Figure 6: Simplified schematic of the all-fiber  $PDL_{\lambda}$  artifact.

fiber (18 dB/m extinction) that provides relatively stable PDL over the range of 15 – 35 °C. The input is a 5 cm section of single-mode (SMF-28) fiber for accurate coupling to system leads. The output section is composed of 40 m of 50/125  $\mu$ m step-index multimode fiber. The high numerical aperture (0.37) of the multimode fiber is sufficient to essentially depolarize the signal,

## Appendix B (Preliminary)

thereby reducing measurement uncertainty arising from output connector and detector PDL, and produces a more accurate calibration. Hot-wire splicing was found to produce the most reliable joints between the dissimilar fibers. The entire length of the splice region was gently immobilized with custom protectors.

This design was chosen initially to provide a simple and relatively inexpensive fabrication method for multiple units. The all-fiber design avoids the usual complications associated with open-beam optics. In practice, one typically trades one set of problems for another. Given the highly stressed nature of polarizing fiber, for example, some sensitivity to variations in the thermal environment can be expected. It was surprising however, to see the magnitude of the variations in PDL with temperature immediately following construction. These variations can easily reach  $\pm 80\%$  of the intended value due, presumably, to shifts in the splice protection assembly. With repeated thermal cycling over the temperature range of  $0 - 50\text{ }^{\circ}\text{C}$ , though, thermal movement usually begins to subside and measured PDL begins to stabilize. This behavior is illustrated in Fig. 7. Additional challenges include reliably splicing dissimilar fibers. Fusion splicers that employ electric arcs were found to be particularly troublesome by causing bubbling of the PZ fiber material. A different splicer using hot-wire heating was found to produce, with the right parameters, a more consistent and better quality splice. Another issue is that of back-reflections at the junctions of dissimilar fibers. When dissimilar fibers are joined, there will be back-reflections due to joint imperfections and to Fresnel reflections at the index boundaries, both of which lead to etalon interference when high-coherence sources are used to

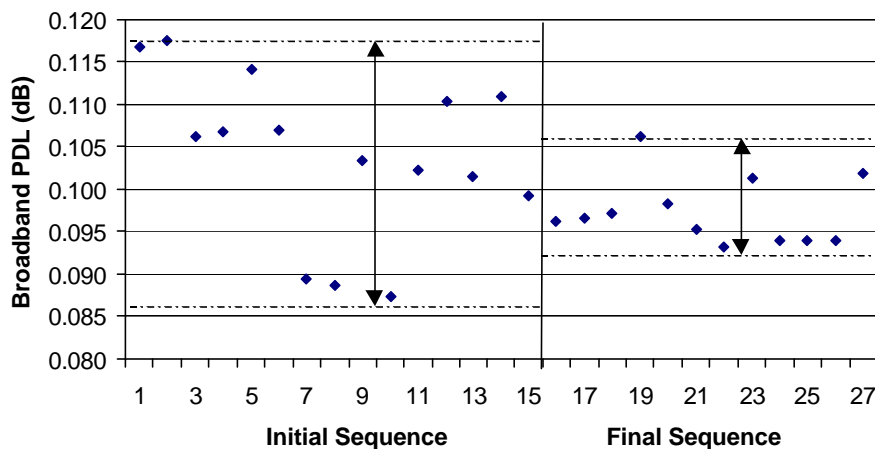


Figure 7: All-fiber artifact temperature variation. The "Initial Sequence" illustrates the thermal instability in PDL before annealing. The "Final Sequence" is the reduced thermal instability after annealing.

## Appendix B (Preliminary)

measure PDL. The level of these reflections can be inferred from the observed interference modulation of  $PDL_\lambda$  as measured with a highly coherent source such as a tunable laser. The magnitude of the modulation,  $\Delta PDL_{\text{mod}}$  (Fig. 8), is approximately 0.25 dB, which can be equated to the fringe contrast of a simple etalon from:

$$\Delta PDL_{\text{mod}} = 10\log((1 - R_j)^2 / (1 + R_j)^2), \quad (4)$$

where  $R_j$  is the reflection at each splice joint. Consequently,  $R_j$  can be solved to yield a reflection of 1.4 % across each joint. This effect precludes the use of these artifacts in measurement systems employing highly coherent sources. In fact, to prevent this effect, one should limit the coherence length  $L_c$  to 10 % of the PZ fiber length (or  $L_c < 1.1$  mm). This coherence length corresponds to a source bandwidth of approximately 0.7 nm (for a source with Lorentzian profile) and is satisfied by our measurement system.

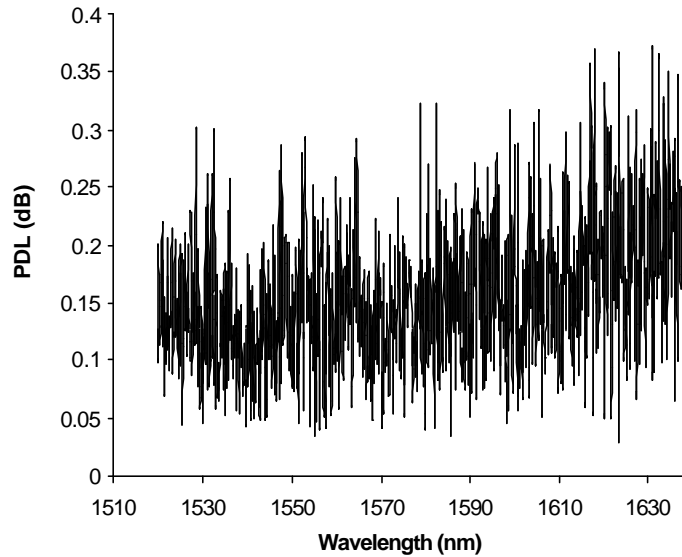


Figure 8:  $PDL_\lambda$  data on a 0.1 dB (nominal) artifact taken using a tunable laser source.

Some recent  $PDL_\lambda$  measurement results from the present system are presented in Fig. 9 for three artifacts. Only selected data points are shown, along with the uncertainties calculated above and a least-squares fit to a fourth-order polynomial. These data span the PDL and wavelength range currently available for transfer via the NIST Measurement Assurance Program.

## Appendix B (Preliminary)

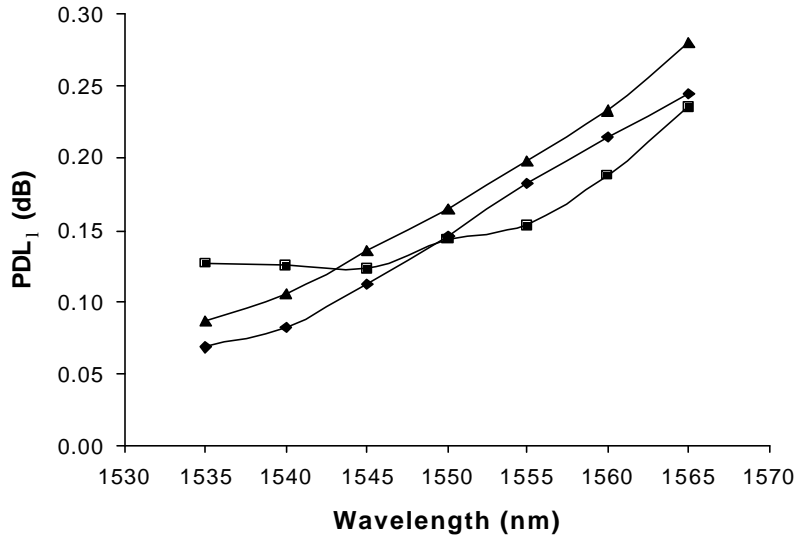


Figure 9:  $PDL_{\lambda}$  for three artifact prototypes with corresponding polynomial least-squares fits.

## 6. Conclusions

An accurate, rapid, non-mechanical technique of characterizing the wavelength dependence of polarization-dependent loss for both single-mode and bulk-optic devices has been developed that offers advantages over more traditional methods. The technique has an expanded uncertainty of 0.0098 dB when measuring a device with 0.12 dB of PDL. A typical measurement scan requires 5 s. Overall accuracy depends on calibration to a primary artifact.

Appendix B  
(Preliminary)

**References**

- [1] M. Gadonna and A. Mabrouki "Polarization Sensitivity Measurements Methods for Passive Optical Components," *Conference on European Fibre Optic Communications and Networks, EFOC&N '93*, The Hague, Netherlands, Technical Digest, pp. 65-67. (1993)
- [2] R. M. Craig, S. L. Gilbert and P. D. Hale, "High Resolution, Nonmechanical Approach to Polarization Dependent Transmission Measurements," *IEEE J. Lightwave Technol.*, vol. 16, pp. 1285-1294, (1998).
- [3] D. Derickson, ed., *Fiber Optic Test and Measurement*. Prentice Hall PTR, 1998, chap 9.5.
- [4] D. L. Favin, B. M. Nyman, and G. Wolter, "System and Method for Measuring Polarization Dependent Loss," *U. S. Patent 5371597*, Dec. 6 1994; B. M. Nyman, D. L. Favin, and G. Wolter, "Automated System for Measuring Polarization Dependent Loss," *OFC '94*, San Jose, California, U.S.A., Technical Digest, pp. 230-231. (1994)
- [5] B. Nyman and G. Wolter, "High-resolution measurement of polarization dependent loss," *IEEE Photon. Technol. Lett.*, vol. 5, pp. 817-818, July (1993).
- [6] S. L. Gilbert, W. C. Swann, and C. Wang, "Hydrogen Cyanide H<sup>13</sup>C<sup>14</sup>N Absorption Reference for 1530 nm to 1560 nm Wavelength Calibration – SRM 2519," *Natl. Inst. Stand. Technol. Special Pub. 260-137* (1998).
- [7] B. N. Taylor and C. E. Kuyatt, "Guidelines for evaluating and expressing the uncertainty of NIST measurement results," *Tech. Note 1297, Nat. Inst. Stand. Technol.*, (1994).
- [8] K.B. Rochford, A.H. Rose, P.A. Williams, C.M. Wang, I.G. Clarke, P.D. Hale, and G.W. Day, "Design and performance of a stable linear retarder", *Applied Optics*, V36, pp. 6458-6465, (1997).



### Qualification of Artifacts and Measurement System

#### Prototype Qualification Prior to Final Assembly

**Low yields in the assembly of the MAP artifact prompted preliminary testing of the artifacts after splicing but before final packaging. This testing is described here.**

The polarizing section is approximately 10 mm of polarizing (PZ) single-mode fiber (18 dB/m extinction). The actual length of the polarizing section can vary somewhat since splices can modify transfer-standard behavior, possibly by introducing additional PDL or changing the rejected-mode extinction. The input is a 5 cm section of common single-mode (SM) fiber for accurate coupling to system leads. The output section is composed of approximately 40 meters of multimode (MM) fiber (50/125  $\mu\text{m}$ , 0.37 NA) to depolarize the signal and reduce uncertainty due to external connector and detector PDL. The MM fiber is wound on a rectangular spool with chamfers of 1.27 cm radius-of-curvature. Hot-wire splicing is used to produce clean joints between the dissimilar fibers. The MM fiber is wound around an aluminum block that also provides a tray for the immobilized polarizing section to reside in. The samples are thermally cycled in an environmental chamber.

All prototype samples are subjected to at least five thermal cycles over the range of 0 – 50 °C to stress-anneal the samples, which serves to either improve or degrade performance. This stress-annealing has been found to be a good indicator of overall stability of the prototype sample. Only those that improve in stability are used as MAP artifacts and are subjected to an additional five thermal cycles over the same range following a 1 week interim resting period that allows the PZ fiber section to equilibrate. The PDL is monitored after each cycle group by an all-states measurement system with a broadband source that detects any instability within the band. Samples are also monitored for high insertion loss and rejected if insertion loss exceeds 3 dB.

Those prototypes that show less than  $\pm 10\%$  variation in PDL following each of the five thermal cycles described above go on to a second round of thermal cycling like that of the first stage with one exception. The testing is now performed with a 1 mW ASE source with a filter centered at 1540 nm that provides a greater signal-to-noise ratio within the band for the all-states measurement. The second round of testing is aimed at isolating those prototypes that settle to within a  $\pm 5\%$  window about the nominal PDL range.

## Appendix C

Prototypes that pass this selection criteria are further immobilized through the use of a thermally conductive, shock-absorbing dielectric gel poured into the tray, covering the PZ fiber section and fiber splices. This gel moderates both temperature gradients and shock loads, both of which lead to potential stress on the active section. The output end of the MM depolarizer section is with a FC/UPC connector for output to a power-meter or photodetector.

At this point, the prototypes are measured for the temperature coefficient of PDL at several wavelengths with the system shown in Fig. 4. This test spans the temperature range 20 to 26 °C ( $23 \pm 3$  °C) and measurements consist of 20-point  $PDL_\lambda$  averages at 5 nm wavelength intervals at both temperature extremes. The resulting slope is calculated to produce the thermal uncertainty as a function of wavelength.

### **Measurement System Qualification**

Specimens that pass all tests to this point are characterized for wavelength dependence of PDL using a 4-state (Mueller/Stokes) matrix method measurement system. This system measures  $PDL_\lambda$  with a standard uncertainty of  $\pm 0.0079$  dB over the 1535 – 1560 nm range.

The first test is designed to check the measurement system calibration. This is done with an assembly that permits the insertion and removal of a BK7 glass Fresnel reflection standard from a collimated beam cavity formed by a high precision, AR-coated asphere that produces a 6 mm beam waist. Without the Fresnel standard assembly in place, the beam is undisturbed and allows a precise baseline to be set. With the assembly in place, the collimated beam is intercepted by an identical asphere that launches the beam into the output MM fiber in with relatively low loss.

The baseline is first taken with source sweep set to the shorter-wavelength range (1535 – 1550 nm). The measurement system is set to average over 20 complete 4-state sequences. The transfer standard assembly is then replaced by the MAP artifact and the system measures  $PDL_\lambda$  another 20 times. This procedure is then repeated five times for an ensemble average.

The entire procedure is now repeated with source sweep set to the longer-wavelength range (1545 – 1560 nm). The region of overlap is checked to ensure results that fall within the expected uncertainty, and the values within the overlap range are averaged.

## Appendix D

### Uncertainties Associated with All-States Measurement

The uncertainties associated with the secondary all-states measurement system used for thermal characterization of PDL<sub>λ</sub> MAP artifact are given in Table 1 for a measurement time of 10 s using Ref. [5]. RSS is defined as the root-sum-of-squares.

Table 1. Estimated expanded uncertainty of the all-states measurement system.

<b>Element Description</b>	<b>Standard Uncertainty</b>
<b>Type A</b>	
Source stability (over 10 s)	0.001 dB
Connector PDL	0.0029 dB
Power meter PDL	0.003 dB
Polarization controller PDL	0.0023 dB
Observed repeatability	0.003 dB
<b>Type B</b>	
Coverage deficiency <sup>5</sup> (5 % of 0.1 dB)	0.0029 dB
Power meter linearity	0.0006 dB
<b>Total <math>u_{AS} = \text{RSS (Type A + Type B)}</math></b>	<b>0.0057 dB</b>

$$\text{Expanded uncertainty} = 2 \times u_{AS} = \mathbf{0.013 \text{ dB}}$$

---

<sup>5</sup> Attempts to cover "all-states" of the Poincaré sphere will be limited by the measurement time and the fraction of the sphere not covered is the "coverage deficiency."

## Appendix E

*Sample Certificate.* *Actual certificate to be sent following MAP measurement*

# National Institute of Standards & Technology

## Measurement Assurance Program

for

### Photometric Polarization-Dependent Loss Measurement in the 1540 – 1560 nm Wavelength Range

This Measurement Assurance Program (MAP) [1] is intended for polarization-dependent loss (PDL) calibration over the spectral range of 1540 nm to 1560 nm. This transfer standard is intended to calibrate only measurement systems that employ photometric methods of PDL determination in transmittance. Photometric methods depend only on the relative variations in transmitted power as a function of polarization state. These methods include pseudo-random all-states [2][3], deterministic all-states [4][5], deterministic fixed-states (Mueller/Stokes) [3][6][7], and enhanced all-states/optical spectrum analyzers (OSA) [2]. The certified value of this transfer standard is not applicable to polarimetric methods such as the Jones matrix analysis of Heffner [8]. In addition, this transfer standard is not certified for PDL calibration in reflection.

This limitation in scope is necessary because the input to this transfer standard is singlemode optical fiber and the output is multimode optical fiber. Consequently, the output has been substantially depolarized in order to reduce the contribution of wavelength-dependent PDL in connectors, components, and detectors that follow the transfer standard in the measurement system. Since polarimetric methods require analysis of the output polarization state, the depolarized output of this transfer standard renders it unsuitable for use with polarimetric methods. This approach was chosen to allow a more accurate calibration of the common measurement systems and is not a judgement on the performance of any polarimetric method.

**Description:** This transfer standard is an all-optical-fiber device that consists of three major elements designed to simulate a wavelength-dependent PDL. The input port is singlemode fiber. The output port is 50/125  $\mu\text{m}$  step-index multimode fiber of high numerical aperture ( $\text{NA} = 0.37$ ), that depolarizes the signal to approximately 5 % degree-of-polarization (when the source bandwidth is  $\geq 1$  nm) to minimize further PDL contributions from connectors and detectors. The PDL is produced by a short section of polarizing fiber that is fusion-spliced between the input and output fiber. The unit is packaged in a small instrument box (approximately 30 cm x 12.5 cm x 9 cm) with FC/UPC fiber connectors for the input and output.

**Limits of Certification:** The certification of this transfer standard is issued when the MAP artifact is returned to NIST, provided the transfer standard meets the criteria outlined in this document throughout the measurement cycle and is stored, handled, and used in accordance with the instructions given. Certification will not be issued if the transfer standard is damaged or otherwise altered or if the transfer standard was subjected to temperatures outside the 0 °C to 50 °C range.

The research and development effort leading to certification was performed by R. M. Craig of the NIST Optoelectronics Division. Statistical consultation was supplied by C.M. Wang of the NIST Statistical Engineering Division. Additional information regarding calculation of uncertainties is found in [1].

## Appendix E

### Sample Certificate. Actual certificate to be sent following MAP measurement

**Certified Values and Uncertainties:** This transfer standard is certified for wavelength-dependent PDL ( $PDL_\lambda$ ), which is the maximum measured polarization-induced change in the insertion loss measured over 1540 nm to 1560 nm.  $PDL_\lambda$  is defined by:

$$PDL_I \equiv PDL(I) = 10 \log \frac{T_{\max}(I)}{T_{\min}(I)} \text{ (dB)}, \quad (1)$$

where  $T_{\max}(I)$  and  $T_{\min}(I)$  are the maximum and minimum transmittance over the entire polarization-state space at wavelength  $\lambda$ .  $PDL_\lambda$  is measured at NIST using a Mueller/Stokes technique.

A locally weighted regression (LOESS) fit [9] is performed on measured  $PDL_\lambda$  data. The fit is used to

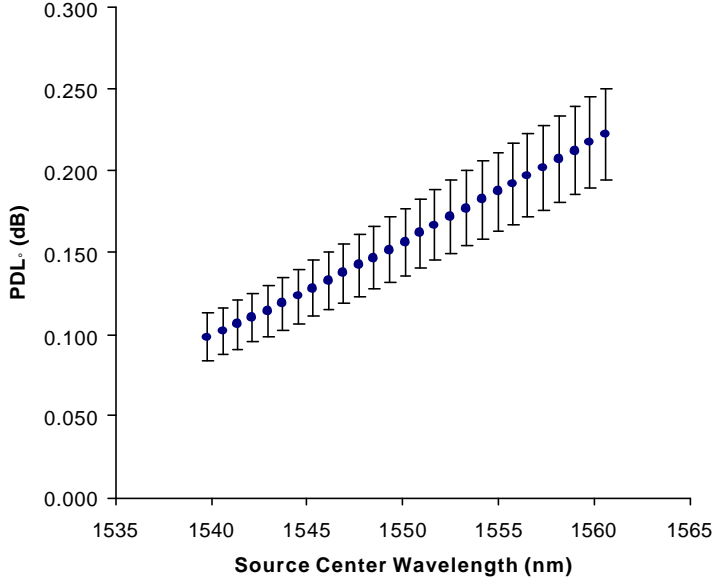


Figure 1. Certified wavelength dependent PDL for MAP transfer standard, including expanded uncertainties for 1 °C.

yield interpolated values (and associated uncertainties) at ITU DWDM grid wavelengths as shown in Fig. 1 and Table 1. The  $PDL_\lambda$  data in Fig. 1 results from two overlapping wavelength scans joined in the overlap region by linear interpolation. The transfer standard is certified at 23 °C and has moderate temperature dependence. This is accounted for as an uncertainty that increases with increasing deviation of measurement temperature from the target 23 °C. The user should choose the uncertainty (23 ± 1 °C or 23 ± 3 °C) that corresponds to the temperature range experienced by the transfer standard during the measurement.

The measurements of wavelength dependence were performed using the NIST  $PDL_\lambda$  measurement system [10] with crosschecks provided by the NIST all-states PDL measurement system using an amplified, spontaneous emission (ASE) source with a 0.7 nm bandwidth tunable filter. The *expanded uncertainties* in Table 1 were calculated in accordance with NIST uncertainty policy [11] as

$$2u_{Tot}(I) = 2\sqrt{u_{MS}^2(I) + \left(u_T \cdot \frac{dPDL(I)}{dT}\right)^2 + \frac{s_{rep}^2(I)}{N} + \left(u_\lambda \cdot \frac{dPDL(I)}{d\lambda}\right)^2 + u_{ship}^2(I) + u_{fit}^2(I)} \quad (2)$$

where  $u_{MS}(I)$  is the standard uncertainty of the NIST  $PDL_\lambda$  measurement system calculated according to [10]. The second term of Eq. 2 is the variance due to thermal dependence.  $u_T = \Delta T / \sqrt{3}$  is the uncertainty associated with the maximum allowed difference ( $\Delta T$ ) of the transfer-standard temperature from the target 23 °C (either 1 °C or 3 °C in Table 1), and  $dPDL(I)/dT$  is the temperature dependence (dB/°C) of the  $PDL_\lambda$  at room temperature (as described below). The derivative term here is approximated by a difference. The next quantity is the variance in the mean of repetitive measurements made on this transfer standard, which establishes the measurement system noise.  $s_{rep}(I)$  is the maximum standard deviation of repetitive  $PDL_\lambda$  scans over wavelength, and  $N$  is the total number of  $PDL_\lambda$  scans used in the certification. The fourth term is the variance due to center wavelength uncertainty.  $u_\lambda$  is the standard

## Appendix E

### Sample Certificate. Actual certificate to be sent following MAP measurement

uncertainty in source center wavelength of the  $PDL_\lambda$  scan range, and  $dPDL(\mathbf{I})/d\mathbf{I}$  is the linear-regression slope of the combined  $PDL_\lambda$  scan (described below). The use of a linear-regression slope rather than an actual derivative is a reasonable approximation here given the relatively small contribution of center wavelength uncertainty. The fifth term,  $\mathbf{u}_{ship}$  is the standard uncertainty assigned to offsets incurred during shipping (described below). Finally,  $\mathbf{u}_{fit}$  is the standard uncertainty associated with the LOESS fitting algorithm. The coverage factor of two is introduced to produce an *expanded uncertainty* for a confidence interval of approximately 95 %.

Table 1. Certified values and expanded uncertainties  
of wavelength-dependent PDL ( $PDL_\lambda$ ) at ITU channel grid frequencies

Central Frequency		Nominal Wavelength $\lambda_0$ (nm)	PDL $_\lambda$ (dB) (LOESS fit)	PDL $_\lambda$ Expanded Uncertainty $2\mathbf{u}_{Tot}$ (dB)	
(THz)	(Channel)			(23 °C $\pm$ 1 °C)	(23 °C $\pm$ 3 °C)
194.7	(16)	1539.77	XXXXXX	XXXXXX	XXXXXX
194.6	(15)	1540.56	XXXXXX	XXXXXX	XXXXXX
194.5	(14)	1541.35	XXXXXX	XXXXXX	XXXXXX
194.4	(13)	1542.14	XXXXXX	XXXXXX	XXXXXX
194.3	(12)	1542.94	XXXXXX	XXXXXX	XXXXXX
194.2	(11)	1543.73	XXXXXX	XXXXXX	XXXXXX
194.1	(10)	1544.53	XXXXXX	XXXXXX	XXXXXX
194.0	(9)	1545.32	XXXXXX	XXXXXX	XXXXXX
193.9	(8)	1546.12	XXXXXX	XXXXXX	XXXXXX
193.8	(7)	1546.92	XXXXXX	XXXXXX	XXXXXX
193.7	(6)	1547.72	XXXXXX	XXXXXX	XXXXXX
193.6	(5)	1548.51	XXXXXX	XXXXXX	XXXXXX
193.5	(4)	1549.32	XXXXXX	XXXXXX	XXXXXX
193.4	(3)	1550.12	XXXXXX	XXXXXX	XXXXXX
193.3	(2)	1550.92	XXXXXX	XXXXXX	XXXXXX
193.2	(1)	1551.72	XXXXXX	XXXXXX	XXXXXX
193.1	(0)	1552.52	XXXXXX	XXXXXX	XXXXXX
193.0	(-1)	1553.33	XXXXXX	XXXXXX	XXXXXX
192.9	(-2)	1554.13	XXXXXX	XXXXXX	XXXXXX
192.8	(-3)	1554.94	XXXXXX	XXXXXX	XXXXXX
192.7	(-4)	1555.75	XXXXXX	XXXXXX	XXXXXX
192.6	(-5)	1556.55	XXXXXX	XXXXXX	XXXXXX
192.5	(-6)	1557.36	XXXXXX	XXXXXX	XXXXXX
192.4	(-7)	1558.17	XXXXXX	XXXXXX	XXXXXX
192.3	(-8)	1558.98	XXXXXX	XXXXXX	XXXXXX
192.4	(-9)	1559.79	XXXXXX	XXXXXX	XXXXXX
192.5	(-10)	1560.61	XXXXXX	XXXXXX	XXXXXX

**NOTE:** All wavelengths are referenced to vacuum. Measurement uncertainties on  $PDL_\lambda$  assume  $\mathbf{u}_\lambda = 0.025$  nm,  $\mathbf{s}_{rep}(\mathbf{I})/\sqrt{10} = 0.0012$  and  $\mathbf{u}_T$  corresponds to either a 23  $\pm$  1 °C or a 23  $\pm$  3 °C temperature uncertainty.

## Appendix E

### Sample Certificate. *Actual certificate to be sent following MAP measurement*

**Instructions for Use:** Make calibrating measurements at a nominal temperature of 23 °C. As discussed in the section on Temperature Dependence (below), the measurement uncertainty increases as the measurement temperature diverges from this 23 °C target. Two temperature tolerances are allowed in Table 1,  $23 \pm 1$  °C and  $23 \pm 3$  °C. For measurement stability, hold the transfer standard at the measurement temperature for at least one hour before making measurements. Make the measurements at one or more ITU wavelengths within Table 1. As described in the section on Input PDL (below), connector variations can lead to fiber-core offsets that produce PDL. Input PDL can cause measurement error so it is recommended that  $PDL_{\lambda}$  be measured as the average of multiple measurements done with a variety of input fiber leads and associated connectors. This helps to ensure random orientations of input PDL axes. As described in the Lead Birefringence section (below), both static and dynamic birefringence in the fiber leads of the measurement system can introduce measurement error in Mueller/Stokes systems. In this case, it is recommended that the pigtail leads be as short as possible and remain rigidly fixed during a measurement. Consequently, Mueller/Stokes systems require somewhat more care to properly calibrate. Finally, the output fiber is a 0.37 NA step-index multimode type with 50/125  $\mu\text{m}$  dimensions. To avoid additional insertion losses, it is recommended that the output fiber lead to the user's detector or measurement system be multimode cable of the same NA. Because the output of the transfer standard is depolarized, calibration uncertainty due to subsequent small ( $<0.05$  dB) connector/detector PDL will be negligible, permitting a more accurate measurement of the transfer standard's value. Calibrate the instrument to the corresponding value from Table 1 using the procedure specified by the instrument manufacturer, c.f. Fig's. 2a and 2b. Wavelength linearity of the instrument can be checked by repeating the procedure at a substantially different ITU channel and comparing it to Table 1.

Care should be taken in making connections to the transfer standard. The bulkhead connectors on the transfer standard unit are the FC/UPC type. When making connections to the transfer standard, use high quality FC/UPC connectors. The cleanliness of the connectors is important. Use a dust-free and residue-free air source and a commercial fiber-endface cleaner before making each connection. If such a cleaner is not available, then use lens paper wetted with reagent-grade alcohol to wipe the ferrule endface and use a clean air source to dry the connector. To retain certification, the transfer standard should not be subjected to temperatures outside the range of 0 °C to 50 °C, and the unit should be stored in a dry environment with long-term temperatures within the range of 15 °C to 35 °C.

**The transfer standard should not be subjected to any mechanical or thermal shocks or strong vibrations and the lid should not be removed. Do not use FC/APC type connectors; otherwise erroneous results and possible connector damage will occur.**

**Input PDL:** Any connection between two singlemode optical fibers can introduce PDL, whether through Fresnel reflections, lateral core offset, or mode-field mismatch. Thus the transfer standard is subject to a PDL uncertainty at the input connection. We have measured connector PDL values in the range of 0.002 – 0.02 dB, but larger values may be possible. In addition, the axis of the input PDL relative to the axis of the internal PDL determines whether it adds or subtracts from the internal PDL. When the axes are aligned, the total PDL will approximate the sum of the two contributions for relatively small values [12][13], and likewise when the axes are orthogonal the total will approximate the difference. There is no way to determine, *a priori*, the relative angle between the two axes. Only by sampling with a variety of input leads and connectors can this uncertainty be reduced by effectively averaging over several axis angles. In addition, use only leads terminated with FC/UPC type connectors.

**Temperature Dependence:** Because the transfer standard uses polarizing fiber, it is sensitive to temperature. The temperature coefficient is individually measured for each transfer standard. The wavelength-dependent temperature coefficient is obtained from  $PDL_{\lambda}$  measurements at 20 °C, 23 °C, and

## Appendix E

### Sample Certificate. Actual certificate to be sent following MAP measurement

26 °C. This temperature dependence has been added in quadrature to the other uncertainties to give the final uncertainty listed in Table 1 for two possible temperature excursions. Also, since the artifact retains some sensitivity to large temperature variations during shipping, an estimate has been made of the

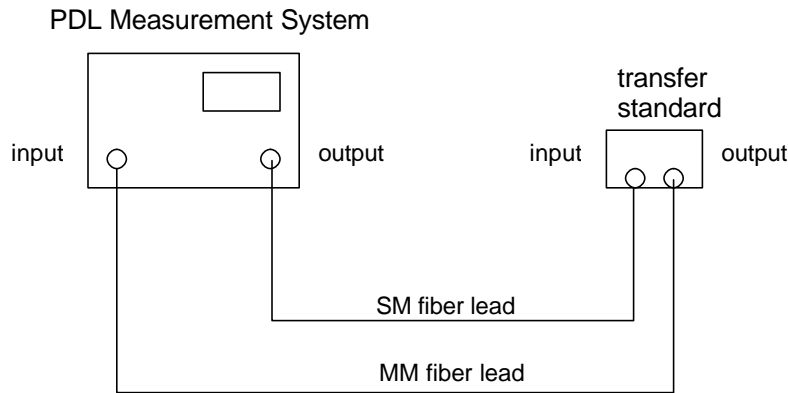


Figure 2a Basic calibration arrangement for all systems.

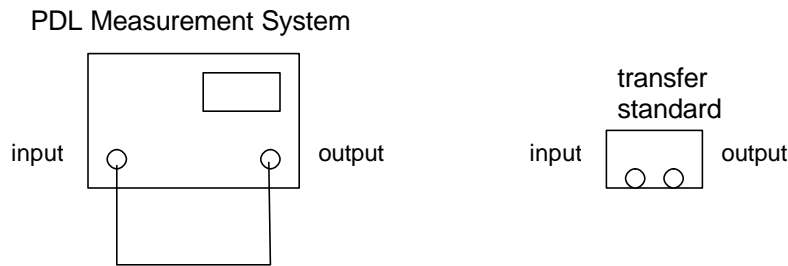


Figure 2b Measurement system baseline.

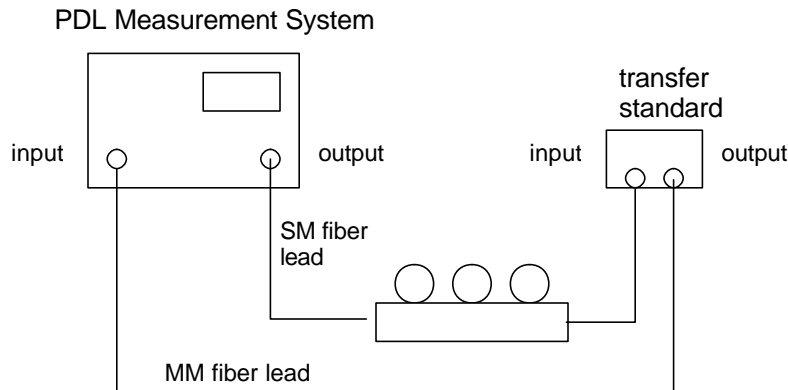


Figure 2c. Mueller/Stokes retardance uncertainty measurement.

uncertainty contribution of  $u_{ship}$ . Based on measured results of simulated shipping conditions, the estimate has been made from the uncertainty contribution as a percentage change in a 0.12 dB nominal reference value. This shift is taken as the adjusted maximum observed shift standard deviation of  $PDL_{\lambda}$  normalized to the wavelength mean of  $PDL_{\lambda}$ , and was found to be 3.5 %. The result (at the 0.12 dB reference value) is calculated to be  $s_{ship} = 0.035 \cdot 0.120 \text{ dB} = 0.0045 \text{ dB}$ . A small logging device attached



## Appendix E

### **Sample Certificate.** *Actual certificate to be sent following MAP measurement*

to each artifact will constantly monitor the temperature environment. Upon return, the thermal history will be analyzed for any temperature excursions outside of the 0 °C – 50 °C range of certification.

**Lead Birefringence:** In the majority of photometric methods, lead birefringence is not an issue as these methods are invariant under Poincaré sphere rotation(s). However, in the case of the four-state Mueller/Stokes measurement, both static and dynamic lead birefringence can impose an uncertainty on the measurement [1]. Large static lead birefringence destroys the required state-space symmetry between (a) initial baseline measurements without the transfer standard in place and (b) the final measurement with the transfer standard in place. The net effect of large static birefringence is to scale the PDL by factors both greater than and less than one. Dynamic lead birefringence in long interconnecting leads alters the baseline PDL level during the course of extended Mueller/Stokes measurements. To minimize this uncertainty, use short, straight leads anchored to a surface for interconnections and limit measurement time between baseline measurements. When short, rigidly mounted input leads are not possible, the orientation of the fiber leads should be randomized between measurements and the measurements should be averaged in order to minimize the lead birefringence effects. Note that the most complete randomization of the leads must include orientations where the fibers do not lie in a single plane as in the case of a fiber-loop polarization controller, c.f. Fig. 2c.

**Optical Source Type:** Because the transfer standard depends on wavelength and because PDL measurements are subject to optical interference arising from multiple reflections, the bandwidth of the source is an important consideration. Very broad sources such as light-emitting diodes (LED) will tend to average (integrate) the transfer standard  $PDL_{\lambda}$  over the bandwidth. Conversely, very narrow sources such as external-cavity-tunable lasers can be precisely adjusted spectrally, but the very long coherence length may lead to very large variations due to interference. In addition, polarizers should not follow polarized sources with pigtail leads, otherwise large power fluctuations may occur. NIST strongly recommends using a stabilized source such as an ASE or edge-emitting LED (EELED) followed by a filter with a 3-dB bandwidth in the range of 0.7 – 20 nm. Note that the filter bandwidth will naturally restrict the range over which the source may be tuned to ensure that no significant power falls outside of the certified wavelength range of  $PDL_{\lambda}$ . Finally, the user should be aware of the additional uncertainty introduced by asymmetry in the source spectra. Refer to App. F of Ref. 1 for a discussion. Source profiles that are significantly different from this simple model must be handled individually.

**Multiple Reflections:** The most probable cause of multiple reflections is poor connections. Use only FC/UPC type connectors cleaned as described in the Instructions for Use section. Dust or dirt in the bulkhead adapter or on the connector ferrule endface can cause multiple reflections across the specimen, which will add noise to the measurement. Other sources of reflection in the measurement system are equally important. If the reflections cannot be reduced, multiple measurements can be made at slightly different wavelength sampling points or temperatures in order to average out the multiple reflection effects.

**Center Wavelength:** Because the wavelength of each  $PDL_{\lambda}$  scan at NIST is registered in real-time to a hydrogen-cyanide gas reference (SRM 2519), wavelength uncertainty is small and limited primarily by the accuracy of fit coefficients obtained during that registration. The standard uncertainty of measurement wavelength for each certified PDL value is 0.025 nm. When multiplied by an observed slope in  $PDL_{\lambda}$  of 0.006 dB/nm, we obtain a standard uncertainty of 0.0015 dB due to wavelength uncertainty.

## Appendix E

### Sample Certificate. Actual certificate to be sent following MAP measurement

#### References

1. Craig, R. M., and Wang, C. M., " Measurement Assurance Program for Wavelength Dependence of Polarization Dependent Loss of Fiber Optic Devices in the 1540 – 1560 nm Wavelength Range," NIST Special Publication 250-60. (forthcoming)
2. D. Derickson, *Fiber Optic Test and Measurement*, Upper Saddle River, NJ: Prentice Hall, 1998.
3. R. M. Craig, S. L. Gilbert, and P. D. Hale, "High-resolution, nonmechanical approach to polarization-dependent transmission measurements," *J. Lightwave Technol.*, vol. 16, pp. 1285-1294, July 1998.
4. N. Mekada, A. Al-Hamdan, T. Murakami, and M. Miyoshi, "New direct measurement technique of polarization dependent loss with high resolution and repeatability." *Tech. Dig., Symp. Optic. Fiber Measurements, SOFM'94*. Boulder, CO, pp. 189-192.
5. M. A. Bhatti and A. S. Siddiqui, "A new polarization dependent loss measurement system," *Int. J. Optoelectronics*, vol. 11, 1 pp. 39-41, 1997.
6. B. Nyman and G. Wolter, "High-resolution measurement of polarization dependent loss," *IEEE Photon. Technol. Lett.*, vol. 5, pp. 817-818, July 1993.
7. D. L. Favin, B. M. Nyman, and G. Wolter, "System and method for measuring polarization dependent loss," U.S. Patent 5371597, Dec. 6, 1994.
8. B. L. Heffner, "Deterministic, analytically complete measurement of polarization-dependent transmission through optical devices," *IEEE Photon. Technol. Lett.*, vol. 4, pp. 451-454, May 1992.
9. Cleveland, W.S. and Devlin, S.J., "Locally Weighted Regression: An Approach to Regression Analysis by Local Fitting," *Journal of the American Statistical Association*, Vol. 83, pp. 596-610. 1988.
10. R. M. Craig, "Accurate spectral characterization of polarization dependent loss." *Tech. Dig., Symp. Optic. Fiber Measurements, SOFM'2000*. Boulder, CO, pp. 113-116.
11. B. N. Taylor and C. E. Kuyatt, "Guidelines for evaluating and expressing the uncertainty of NIST measurement results," Tech. Note 1297, *Nat. Inst. Stand. Technol.*, 1994.
12. N. Gisin, "Statistics of PDL," *Opt. Comm.*, vol. 114, pp. 399-405, 1995.
13. A. Elamari, N. Gisin, B. Perny, H. Zbinden and C. Zimmer, "Statistical prediction and experimental verification of concatenations of fiber optic components with polarization dependent loss," *J. Lightwave Technol.*, vol. 16, pp. 332-339, 1998.

## Effect of Source Spectral Symmetry

Given the significant dependence of PDL on wavelength, the user may find it important to consider not only the source bandwidth but also the spectral symmetry across that bandwidth. It is possible for asymmetry of the source spectrum to cause PDL measurement errors. Refer to Fig. 1 for an example of a simple, triangular asymmetry in the source spectrum. Here one can clearly see that the spectral intensity peak,  $P_0$  (dB), is offset from the center and that a spectral slope,  $m_s$  (dB/nm), can characterize the asymmetry. Given that an asymmetric (non-zero-slope) source spectrum will shift the integrated average  $PDL_\lambda$  away from the midpoint of the  $\lambda$ -averaging range, it is possible to establish a maximum permissible spectral slope. A negative spectral slope will weight the integrated average  $PDL_\lambda$  towards shorter wavelengths, while a positive slope will weight the average towards longer wavelengths. The maximum spectral slope (over a 3 dB bandwidth) allowable to maintain a 1 % uncertainty is calculated to be  $m_s \pm 0.2$

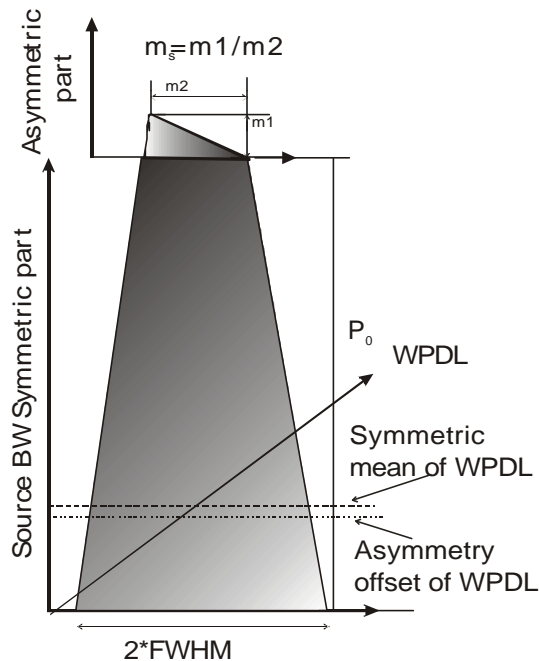


Figure 1. Illustration of the effect of a simple, triangular, source spectral asymmetry. Note that a symmetric filter will integrate the spectral PDL to the midpoint value and that the asymmetric component will contribute a small offset.

dB/nm while the maximum slope to maintain a 3 % uncertainty is  $m_s \pm 0.6$  (dB/nm). For a 0.12 dB reference value, this leads to a standard uncertainty contribution of 0.0018 dB. There are, of course, more general cases that must be dealt with individually. These include source spectra for which the asymmetry is not well represented by a slope. To minimize this effect, the user should verify that the source spectrum is symmetric about the peak.

## Appendix G

### **Shipping and Handling Instructions**

Because the transfer-standard assembly retains some sensitivity to thermal and mechanical shock, it is shipped as rapidly as possible in a specially padded and insulated shipping container. We request and strongly recommend that this container be reused for the return shipment as it is very protective and helps to assure continued certification. The assembled units contain a temperature-logging device on the back panel that the user should be aware of but, in general, not concerned with. This logging device will monitor the temperature environment during shipment and use.

This page intentionally left blank

# Appendix H

## PDL<sub>1</sub> Artifact Tray/MM Depolarizer Mount

The following is a schematic of the aluminum artifact mounting tray and depolarizer spool. Units given are in inches rather than SI. The upper tray holds the fiber splices as well as the immobilizing gel. It is important to note the dimension of the spool's radii of curvature.

